Atmos. Meas. Tech. Discuss., 5, 8925–8967, 2012
www.atmos-meas-tech-discuss.net/5/8925/2012/
doi:10.5194/amtd-5-8925-2012

Atmospheric Measurement Techniques Discussions

Measurements of air pollution emission factors for marine transportation

B. Alföldy[1], J. Balzani Lööv[1], F. Lagler[1], J. Mellqvist[2], N. Berg[2], J. Beecken[2], H. Weststrate[3], J. Duyzer[3], L. Bencs[4,5], B. Horemans[4], F. Cavalli[1], J.-P. Putaud[1], G. Janssens-Maenhout[1], A. Pintér Csordás[6], R. Van Grieken[4], A. Borowiak[1], and J. Hjorth[1]

[1]European Commission, Joint Research Centre, Ispra (VA), Italy
[2]Chalmers University of Technology, Göteborg, Sweden
[3]The Netherlands Organization for Applied Scientific Research, Utrecht, The Netherlands
[4]Department of Chemistry, University of Antwerp, Antwerp, Belgium
[5]Institute for Solid State Physics and Optics, Wigner Research Centre for Physics, Hungarian Academy of Sciences, Budapest, Hungary
[6]Centre for Energy Research, Hungarian Academy of Sciences, Budapest, Hungary

Received: 14 October 2012 – Accepted: 14 November 2012 – Published: 20 December 2012

Correspondence to: B. Alföldy (balint.z.alfoldy@gmail.com)

Published by Copernicus Publications on behalf of the European Geosciences Union.

Abstract

The chemical composition of the plumes of seagoing ships was investigated during a two weeks long measurement campaign in the port of Rotterdam, Hoek van Holland, The Netherlands, in September 2009. Altogether, 497 ships were monitored and a statistical evaluation of emission factors (g kg^{-1} fuel) was provided. The concerned main atmospheric components were SO_2, NO_2, NO_x and the aerosol particle number. In addition, the elemental and water-soluble ionic composition of the emitted particulate matter was determined. Emission factors were expressed as a function of ship type, power and crankshaft rotational speed. The average SO_2 emission factor was found to be roughly half of what is allowed in sulphur emission control areas (16 vs. 30 g kg^{-1} fuel), and exceedances of this limit were rarely registered. A significant linear relationship was observed between the SO_2 and particle number emission factor. The intercept of the regression line, 0.5×10^{16} (kg fuel)$^{-1}$, gives the average number of particles formed during the burning of 1 kg zero sulphur content fuel, while the slope, 2×10^{18}, provides the average number of particles formed with 1 kg sulphur burnt with the fuel. Water-soluble ionic composition analysis of the aerosol samples from the plumes showed that ~ 144 g of particulate sulphate was emitted from 1 kg sulphur burnt with the fuel. The mass median diameter of sulphate particles estimated from the measurements was ~ 42 nm.

1 Introduction

Although shipping in general is a very energy efficient way to transport goods, the increase in international ship traffic and the relatively high SO_x ($SO_2 + SO_3$) and NO_x ($NO + NO_2$) emission factors (EFs) of ship engines raised concerns on the impact of these emissions on the environment and human health. The contribution of ships to global NO_x emissions is about 15 %, while 4–9 % of the global SO_2 emissions can be attributed to ships (Eyring et al., 2010). Due to its significant contribution to the

AMTD
5, 8925–8967, 2012

anthropogenic SO_2 emission, global shipping might also play an important role in climate change. While radiative forcing (RF) of shipping generated CO_2 is only 2 % of the total anthropogenic CO_2 RF, the direct aerosol (cooling) effect of shipping emitted sulphate is about 8 % of the total anthropogenic direct aerosol RF. In addition, some calculations estimate that shipping related indirect aerosol effects can exceed 40 % of the total indirect aerosol effects of anthropogenic sources (Eyring et al., 2010). Since the sulphur content of heavy fuel oil will be radically decreased in the coming years, its climatic consequences must also be considered. On the other hand, any decrease in the global SO_2 emission is generally beneficial for the environment and human health. SO_2 emissions increase the acidity of the atmosphere, thereby damaging living organisms and producing acid rain (IPCC, 2007). In addition, the secondary formed sulphate aerosol contributes to the PM load, which adverse health effect on humans is well documented (Cohen et al., 2005; Cofala et al., 2007; Corbett et al., 2007). The complexity of the environmental effects of atmospheric SO_2 requires accurate consideration of ship emissions in the light of mitigation policies.

Sulphur is a mineral constituent of crude oil, ranging from 0.5 up to 5 % by mass, depending on the quality of the oil. During combustion of crude oil, the mineral sulphur is oxidised mainly to SO_2 and in minor quantities to SO_3 and sulphuric acid.

Nitrogen oxides (NO_x) are also emitted during combustion as a result of the oxidation of atmospheric N_2 and the small fraction of nitrogen in the fuel. NO_x contributes to acidification and to the formation of tropospheric ozone, which can be harmful for human health and vegetation.

Atmospheric emissions from ships have not been the focus of regulations until recent years; the lack of regulations allowed the use of heavy fuel oil (HFO), the residue with a typical high sulphur content which remains after refining crude oil. Also the emissions of nitrogen oxides from ships have not been regulated until recently.

As a result of the harmful environmental effects related with the combustion of HFO, the International Maritime Organization (IMO) regulated the sulphur content of the fuel (MARPOL Annex VI) and NO_x emission rates through the Annex VI of the MARPOL

AMTD
5, 8925–8967, 2012

protocol, which entered into force in 2005. At the time of this study, the global limit for all seas and oceans was 4.5 %, except in Sulphur Emission Control Areas (SECAs), where it was 1.5 %. These limit values will change in the near future; in 2012, the global 4.5 % will be reduced to 3.5 %, from which it will be reduced to 0.5 % by 2020; the 1.5 % in SECAs was reduced to 1 % in 2010 and will be further decreased to 0.1 % from 2015 onwards (Fig. 1).

In the case of NO_x, the engine power-weighted emission rate is limited by the MARPOL rules. This regulation is more complex, since the limit depends on the fuel efficiency of the used engine. Large ships, such as container vessels and tankers usually run with slow speed engines with a rated engine speed of around 100 rpm. These ships are fuel efficient (down to 160 g kWh^{-1}), but due to the long residence time of the gas in the combustion space they produce high amounts of NO_x. Ferries and intermediate sized ships usually use medium speed engines with a rated engine speed of around 500 rpm. These engines are less fuel efficient (180–200 g kWh^{-1}), but on the other hand produce less NO_x compared to the slow speed engines. Ships built after 2000 have to fulfil the IMO Tier I emission values regarding NO_x, and by 2011 the emission for new ships should be even 20 % lower (Tier II, see Fig. 2). Also, ships built between 1990 and 2000 will be forced to retrofit NO_x abatement equipment, if a cost effective upgrade is available. Tier III is not yet ratified, but this limit will become valid in special NO_x emission control areas (NECAs) and for ships built during or after 2016.

Due to its important environmental impact, the number of ship emission studies is growing year by year. In the present work we use results of Hobbs et al. (2000), Sinha et al. (2003), Chen et al. (2005), Agrawal et al. (2008), Petzold et al. (2008), Moldanova et al. (2009) and Murphy et al. (2009). These studies provide a comprehensive description of ship emissions; however, due to the experimental difficulties they could focus on only one or two particular ships. These studies demonstrate that the emission rates are highly variable between the ships. For this reason the contribution of marine transportation to the global budget of air pollutants can only be assessed based on a statistically representative fleet. Despite the high international interest, only a few

AMTD
5, 8925–8967, 2012

statistically representative studies have been performed so far (see e.g. Williams et al., 2009; Lack et al., 2009). This work aimed at reducing the white spots on the map and characterise the ship emission statistically in a special area, i.e. in the SECA. However, the results can be extrapolated for the global shipping, as we present relationships between the fuel sulphur ratio and SO_2 and sulphate EFs. Scaling up by the fuel sulphur ratio, globally valid EFs can be derived, while emission factors for NO_x and non sulphuric particles can be considered as globally valid values as they depend only slightly on fuel type (see discussion below).

Some of the co-authors applied previously in situ plume measurements, as discussed in detail below. The Netherlands Organization for Applied Scientific Research (TNO) organized several short measurement campaigns at the coast of the North Sea in order to retrieve real EFs of ship combustion processes (Duyzer et al., 2006; Segers and Duyzer, 2007). Chalmers University of Technology performed in situ plume investigation campaigns in the Baltic region with similar purposes (Mellqvist et al., 2008, 2010). In these studies (as in the present work) EFs for NO_x, SO_2 and particulate matter (PM) were retrieved. In addition, knowing that the majority of the fuel sulphur content is emitted as SO_2, the sulphur content of the fuel can be derived from the SO_2 EF. This can be an efficient tool in hands of authorities to check the sulphur limit compliance of the ships remotely, without boarding and taking fuel samples.

2 Experimental

2.1 Measurement campaign

A two-week measurement campaign was conducted at the shores of the entrance channel to the Port of Rotterdam in Hoek van Holland, The Netherlands. In order to catch the exhaust plumes of the passing ships on the downwind shore of the channel, the sampling location was flexibly switched according to the wind direction. One sampling location was selected at the northern side of the "Nieuwe Waterweg" (HvH), while

AMTD
5, 8925–8967, 2012

another was chosen on a land stretch at the southern side, designated as “Landtong” (LG, Fig. 3). Additionally, a location at the “Maasvlakte”(ME), at the extreme south-western side of the channel has been used once. It should be mentioned that the traffic at the entrance of the channel is split into two: the most frequently sampled northern channel is connected inlands to the city of Rotterdam, while the southern leads to several petrol and food terminals and the Europort.

The measurements were concurrently performed by three independent mobile laboratories of the Joint Research Centre (JRC), TNO and Chalmers, each of them being deployed in vans. All of these labs were equipped with a complete air quality monitoring system for the measurement of CO_2 and gaseous air pollutants (SO_2, NO_2 and NO_x) at 2–5 m above the ground. In addition, JRC measured SO_2 and CO_2 by a parallel system at 15 m above the ground, as well as the total aerosol number concentration at ground level ($\sim$ 1 m). Aerosols were also sampled for chemical analysis as described below. Besides these fixed point measurements, the group of Chalmers performed chasing measurements by a coast guard helicopter and a port service boat. The results of these measurements are reported in other papers (Mellqvist et al., 2011; Berg et al., 2012).

During the campaign, the measurement systems were running continuously, except while moving the labs from one sampling point to the other. The identification of the ships was performed by human observations during daytime. Particular care was paid to annotate AIS (Automated Information System) information on the ships sailing by (speed, IMO number, distance, ships’ characteristics).

2.2 Instrumentation

SO_2 concentrations were monitored using a THERMO ELECTRON model 43C Trace Level UV fluorescent analyser (Thermo Electron Corporation, Franklin, MA, USA). The intensity of the fluorescent radiation, detected by a photomultiplier tube, is proportional to the SO_2 concentration sampled in the ambient air. However, other atmospheric gases, such as NO and polycyclic aromatic hydrocarbons (PAHs) are also fluorescing,

AMTD
5, 8925–8967, 2012

hence they can cause interference on the determination of SO_2. NO concentrations may lead to a bias in the results typically from the order of 2–3 % of the NO reading, hence 100 ppmv NO will be interpreted as 2–3 ppmv SO_2, this was corrected during the data treatment. The interference by PAHs was avoided by a "hydrocarbon kicker". In order to achieve the required response time, the diameter of the critical orifice had to be enlarged to allow a faster sampling flow ($\sim 1.5\,L\,min^{-1}$). Also the time constant in the software of the SO_2-analyzer was set to 1 s. With these settings, the response time (t_{90}) of the instrument was around 15 s. For calibration, a reference gas mixture of 100 ppbv SO_2 in synthetic air was applied, while SO_2-free synthetic air was used for the baseline (zero) calibration. Instrument accuracy: ±10 %.

CO_2 concentrations were measured using a LI-COR LI-7000 (LI-COR Biosciences, Lincoln, NE, USA) optical instrument, which measures infrared absorption in two wavelength bands around 5 µm, using a broadband light source and band pass filters. In these wavelength bands, both H_2O and CO_2 absorb the radiation rather strongly. In order to overcome this interference, the instrument includes two cells. One is used for the sample and the other as a reference cell, containing known concentrations of CO_2 and H_2O. The CO_2 concentration in the sample cell is obtained by calculating the light absorption, due to CO_2 and H_2O by comparing the intensities in the sample and reference cells. The calibration curve was checked by a span gas calibration with three known CO_2 gas concentrations in the measurement range (i.e., 370, 395, 420 ppmv). The air sampling flow rate of the LI-COR instrument is around $6\,L\,min^{-1}$, while the flow for the reference gas is $150\,mL\,min^{-1}$. Depending on the pump speed, this instrument can have a faster response than the SO_2 analyzer, i.e., the t_{90} is lower than 5 s. For calibration, a single analytical standard mixture of CO_2 in air (395 ppmv), together with nitrogen (less than 1 ppmv CO_2 content) is needed as a gas for the reference cell and zero calibration respectively. Instrument accuracy: ±0.08 ppm.

The NO-NO_x measurement was performed by a THERMO ELECTRON model 42C (Thermo Electron Corporation, Franklin, MA, USA) that measures NO by the chemiluminescence reaction between ozone and NO. Normally, the instrument works in a dual

AMTD
5, 8925–8967, 2012

channel principle. In one channel, the air passes for some seconds through a heated Mo-catalyst (which converts NO_2 to NO), and hence, the resulting signal represents the sum of NO and NO_2 (NO_x). In the second channel, NO is measured exclusively by bypassing the Mo-converter. In order to increase the response time to a t_{90} of about 15 s, the time constant was changed to 1 s. This setting does not allow for the measurement of NO and NO_x together. Therefore, two identical instruments were used, one measuring NO and the other measuring total NO_x. For calibration, a reference gas mixture of around 200 ppbv NO in N_2 was applied. Instrument accuracy: ±10 %.

Particle counting was performed by a TSI 3007 portable CPC (TSI Incorporated, Shoreview, MN, USA). The device operates in the 0.01–1 µm size range and the 0–100 000 cm^{-3} concentration range, which is suitable for ship plume measurements. During the measurements, the device was never saturated by an excessive number of particles. Instrument accuracy: ±10 %.

Size-segregated particulate matter was collected with an MS&T™ impactor (Air Diagnostics and Engineering Inc., Harrison, ME, USA) at an aerosol size-range of PM_{10}. Pallflex-type TK15-G3M membrane filters (Pall Life Sciences, Ann Arbor, MI, USA) with 0.3 µm pore-size and 37 mm diameter were applied. Each impactor unit was attached to a vacuum pump (Air Diagnostics and Engineering Inc.), operated at a flow-rate of 10 L min^{-1}. The air-flows were checked daily with a calibrated rota meter. The sampled air volume was registered with standard gas meters.

Independent filter sampling was performed during ship plume events (plume filters) and between the plume events (background filters). These events were clearly recognized by observing the sharp increase of CO_2 level after the passing of a ship upwind to the monitoring point. The difference between plume and background filter concentrations provides the species' mixing ratio in the plume.

Since the amount of aerosol sampled during a single plume event (duration: max. 3–4 min) was not enough for chemical analysis, the aerosols of several plume events were collected on each "plume" filter. Thus, a PM_{10} "plume" filter corresponds roughly to one day average emission of the ships (average of 37–75 ships).

AMTD
5, 8925–8967, 2012

The aerosol-loaded filters (plume and background) were subjected to secondary target X-ray fluorescence analysis (XRF), for the determination of elemental content of the samples (especially focusing on Ni and V, which are atmospheric tracers of heavy oil combustion). The measurement was implemented by a tube excited XRF system using a SIEMENS diffraction tube with Mo anode and Mo secondary target. The fluorescence spectrum was recorded by a KETEK AXAS-A X-ray detector (KETEK GmbH, Munich, Germany). For quantitative analysis, the sensitivity curve of the measurement system was recorded by measuring a series of standard thin Ni and V foils (NIST, Gaithersburg, MD, USA).

Since XRF analysis is considered to be a non-destructive analytical technique, the samples measured by XRF could be subject to further alternative analysis. Ion chromatography (IC) analysis was performed on the filters by a Dionex Model DX-120 (Dionex, Sunnyvale, CA, USA) ion chromatograph, equipped with Dionex IonPack CS16 cation and AS14 anion exchanger columns and a CDM-3 conductivity detector. For sample introduction, both the standard and sample solutions were injected through a 20 µL loop. The eluents applied for the anion and cation exchangers were 3.5 mM Na_2CO_3 plus 1.0 mM $NaHCO_3$, and 17 mM H_2SO_4, respectively. The flow rates were 1.2 and 1.0 mL min^{-1} for the anion and the cation column, respectively. For suppressing the conductivity of the eluent, the ASRS-300 and CSRS-300 ULTRA suppressors were applied for the anion and cation exchanger, respectively. Calibration was made against two sets of multi-ion standard solutions, each consisting of five solutions of either the anions or the cations, respectively. Three replicate measurements were performed for each sample/standard solution, from which data the average value and the standard deviation was calculated. The precision of the determinations for each analysis was better than 3.6 %. Certified Multianion and Multication Standard Solutions of PRIMUS (Sigma-Aldrich, 210 Steinheim, Switzerland) as reference materials were applied for verifying the accuracy of the IC method.

The filters were exposed to ultrasonic aided leaching in 5 mL ultrapure water (Milli-Q) in a Bransonic Model 2210 ultrasonic bath (Branson, Danbury, CT, USA). Each

AMTD
5, 8925–8967, 2012

leachate solution was filtered through a Millex-GV syringe driven filter unit (Millipore, Carrigtwohill, Co. Cork, Ireland) with 0.22 µm pore size to prevent any particles entering the IC columns. The leachates were analysed for their cationic and anionic content. Field blank filters were also analysed and used for blank corrections.

2.3 Calculation of emission factors

Emission factors of the components were calculated (in g emitted per kg fuel) for each detected plume passage. When an emission plume passed over the sampling point, the concentration peaks of pollutants were registered by the instruments. For EF calculation, the net peak areas were used (time integral of the concentrations). To generate the net peak area, a properly considered background is needed. For this purpose, the 1–2 min averages of the concentrations before and after the plume events were taken, and their average values as a background concentration were subtracted from the total peak area.

Considering the molecular weight of carbon and sulphur dioxide, and the carbon mass percent in the fuel (87 ± 1.5 %; Cooper et al., 2005) the SO_2 EF can be expressed as:

$$\mathrm{EF}[\frac{\mathrm{g}}{\mathrm{kg}}] = \frac{C(SO_2)[\mathrm{ppb}\cdot s]}{C(CO_2)[\mathrm{ppb}\cdot s]}\cdot\frac{64}{12}\cdot 0.87\cdot 1000 = \frac{C(SO_2)[\mathrm{ppb}\cdot s]}{C(CO_2)[\mathrm{ppb}\cdot s]}\cdot 4640, \quad (1)$$

where $C(...)$ is the net time integral of the component's mixing ratio (over the background).

Since most of the fuel's sulphur content is emitted as SO_2, the SO_2 EF can be converted to the fuel's sulphur content:

$$s[\%] = \frac{32}{64}\cdot \mathrm{EF}\times 10^{-1} + R = \frac{1}{20}\cdot \mathrm{EF} + R, \quad (2)$$

where R represents the sulphur content that is emitted in other forms than SO_2 (SO_3 or particulate sulphate). This amount is generally lower than 6 % of the fuel sulphur ratio (see Table 3).

AMTD
5, 8925–8967, 2012

The NO_x EFs can be calculated based on the total nitrogen oxide concentration ($NO + NO_2$, expressed as NO_2 equivalent) compared to the CO_2 concentration. Considering the molecular weights of these compounds and the mass percentage of carbon in ship fuel, the NO_2 equivalent EF can be calculated as follows:

$$EF[\frac{g}{kg}] = \frac{(C(NO)[ppb \cdot s] + C(NO_2)[ppb \cdot s]) \cdot 46}{C(CO_2)[ppb \cdot s] \cdot 12} \cdot 0.87 \cdot 1000. \quad (3)$$

Particle EFs, as well as element and water-soluble ionic EFs were also calculated based on their plume concentration normalised by the CO_2 concentration. In case of element and ionic EF, integration of several subsequent CO_2 peak areas was necessary as it was described above.

3 Results and discussion

During the campaign, altogether 497 plumes of 341 ships were measured. About half of the plumes were measured in a single case (only TNO), the other half in three or four cases (TNO + 2 JRC + Chalmers). If a plume was measured in multiple cases, average values were considered and the standard deviation was applied for uncertainty estimation. The average relative standard deviation (SD) of SO_2 and NO_x EF was 23 % and 26 % respectively. These uncertainty values are composed of the errors of the concentration measurements (for SO_2, NO_x and CO_2, see Sect. 2.2), and the calculation uncertainties (i.e., peak area calculation, background consideration).

Some ships plumes were measured twice or more times during the campaign (e.g., Stena Line ferries two times each day, or port service ships many times a day). The average SD for the repeated SO_2 EF measurement was 30 %, while that of NO_x EF measurement was 34 %. These SD values are slightly higher than the uncertainty of a single measurement. Considering that the circumstances of different emissions of a certain ship (fuel type, engine operating conditions etc.) were not necessarily the same, these SD values demonstrate good repeatability of the measurements.

AMTD
5, 8925–8967, 2012

The distribution of the measured ships as a function of their duty type is presented in Fig. 4. As a comparison, information on the activity data and technology share of global bottom-up emission inventories, such as EDGARv4.2 (European Commission, 2011) were consulted, and the predicted distribution of duty types are presented in the figure. The EDGARv4.2 uses the bunker statistics of the International Energy Association (IEA) as input for the activity data and differentiates between the presences in ports and at sea based on Dalsoren et al. (2009). The EDGAR database associates for its international sea transport a high share to tanker, cargo, container ships and bulk carriers. Our finding verifies this apportionment of the global fleet, except the high contribution of bulk carriers, which appears with low frequency in the measurement results. It can be ascribed to the fact that these ships generally berth in Europort using the southern channel (see Fig. 3), thus they could be sampled from the ME location only for one day of the campaign. Further, EDGAR database does not take into account Inland and Patrol Vessels.

It is to be mentioned that tankers, bulk carriers and container ships are also cargo ships. In this study, multipurpose ships are called "cargo ships" if they can carry containers and dry-bulk goods, while the term of "container ship" covers the fully cellular types of cargo ships. The term "tanker" covers all types of ships carrying liquids and/or gases.

3.1 SO_2 emission factor

Figure 5 shows the distribution of SO_2 EFs among the ships. The entire SO_2 EF range was divided into 24 bins and the frequencies of the bins plotted along the y-axes. The distribution is bimodal, which indicates the existence of two ship classes with different SO_2 emission characteristics. In the lower mode, the EF is lower than 6 g (kg fuel)$^{-1}$ which corresponds to a sulphur-to-fuel ratio less than 0.3 % (see Eq. 2). The low mode contains service and port authorities' ships, such as patrol vessels, tug boats and suction hoppers (local activity), as well as inland vessels that use low sulphur fuel. The high mode has a maximum around 14–18 g (kg fuel)$^{-1}$ (0.7–0.9 %) which is lower than

AMTD
5, 8925–8967, 2012

the actual SECA emission limit value by 50–40 %. This class is formed by container and cargo ships, tankers and ferries (RO-RO, i.e. roll on-roll off passenger and cargo) that have generally one or more main engines for propulsion, and several auxiliary engines for manoeuvring and energy production. While main engines generally run on HFO with the allowed sulphur content (it was 1.5 % in SECA at the time of the study), auxiliary engines use lower sulphur fuels, marine diesel oil (MDO) or distilled diesel oil. The resultant SO_2 EF is determined by the high EF of main engines and the low EF of auxiliary engines. Consequently, the resulting EF is always lower than the EF of the main engine, depending on its relative contribution to the total emission. Typical contribution of auxiliary engine's fuel consumption in the total fuel consumption is about 10 % at sea (Endersen et al., 2007; Whall et al., 2007), but can grow up to 45 % during manoeuvring in ports (Whall et al., 2007). Taking these contribution values and assuming 0.5 % and 1.5 % sulphur content of MDO and HFO respectively, the reduction of the total SO_2 EF caused by auxiliary engines' contribution can be estimated as 6 % at sea and 30 % in ports.

Since our measurements were taken at the entrance of the port, various contributions of auxiliary engines should be considered from 6 to 30 %. Consequently, the higher EF mode is quite wide, including ships with an SO_2 EF between 8–30 g (kg fuel)$^{-1}$. Only seven ships were found with an EF above 30 g (kg fuel)$^{-1}$, corresponding to a fuel sulphur content higher than 1.5 % (SECA limit). Thus the number of exceedances was less than 2 % of the total number of observations.

Figure 6 shows the SO_2 EF distribution according to the duty type of the ships. One can distinguish three SO_2 emission ranges. The first, formed by inland vessels, for which the average EF is ~ 1 g (kg fuel)$^{-1}$ (0.05 % sulphur fuel content). These ships use distilled diesel fuel. The second class contains port service ships like patrol vessels and tug boats with a 4–6 g (kg fuel)$^{-1}$ EF on average. Sea duty ships form the third class, with EFs ranging from 10 to 16 g (kg fuel)$^{-1}$ on average.

Figure 7 shows the SO_2 EF distribution against the operational crankshaft rotational speed. Since the crankshaft-rotational speed distribution followed a lognormal trend,

AMTD
5, 8925–8967, 2012

the whole range from 80 to 2100 rotations per min (rpm) was divided into 11 intervals based on a logarithmic scale. Borders of the rpm intervals are written along the x-axis. Ranges of 2 strokes and 4 strokes engines are marked. Inland vessels were excluded from the distribution, since they form a distinct SO_2 EF class.

As it can be seen in the figure, there is no overlapping between rotational speed ranges of two stroke and four stroke engines, and no significant difference can be observed for SO_2 EFs between the two engine types. Below 700 rpm the SO_2 EF is 13–14 g (kg fuel)$^{-1}$, independently from the stroke number of the engine. Between 700 and 980 rpm, the SO_2 EF gradually decreases down to 1–2 g (kg fuel)$^{-1}$. Most of the port service ships that use low sulphur content fuel have high speed engines. These ships form the last three classes, with engine speed higher than 980 rpm.

The engine power of the studied ships ranged from 400 to 80 000 kW, following a lognormal distribution. The power range was divided into 8 intervals based on a logarithmic scale. The average SO_2 EF of each power bin is plotted along the y-axes of Fig. 8. The first two intervals with low EFs refer to the local activity ships that generally have engines with low or moderate power. Over 1800 kW, the EF jumps over 10 g (kg fuel)$^{-1}$ and then gradually increases up to 16 g (kg fuel)$^{-1}$. The reason for the obviously growing trend of SO_2 EF in the 1800–80 000 kW range is not clear; it might be explained by the decreasing contribution of auxiliary engines to the total emission. The higher the power of the main engine, the lower the relative contribution of auxiliary engines, which eventually causes a higher SO_2 EF.

Following the EMEP/EEA 2009 (CORINAIR) recommendations EDGARv4.2 classifies the different vessel types in two categories: (1) the low momentum (power) category, grouping Local Activity, Tug Boat and Suction Hopper, and (2) the high momentum (power) category, grouping the rest. The CORINAIR estimates 10 g (kg fuel)$^{-1}$ SO_2 EF for category (1), while 52.5 g (kg fuel)$^{-1}$ SO_2 EF for category (2) as a global average (including SECA). These two categories can be identified in Figs. 6 and 8, with obviously lower SO_2 EF, since our measurements were performed in SECA. The gap between

AMTD
5, 8925–8967, 2012

category (1) and (2) is about fivefold in EDGARv4.2, while we found only threefold increase according the lower sulphur limit at SECA.

3.2 Particle emission factor

Since a minor part of the sulphur content of the fuel is emitted in particulate form, the distribution of the particle EF is similar to that of SO_2 (Fig. 9). As for SO_2, the emission factor distribution is bimodal, with a maximum at 0.8×10^{16} (kg fuel)$^{-1}$ (low sulphur fuel) and 1.8×10^{16} (kg fuel)$^{-1}$ (high sulphur fuel). Sinha (2003) reported particle EFs for ships in the range from 1.2–6 $\times 10^{16}$ (kg fuel)$^{-1}$, which covers the higher mode of the present results.

Average particle and SO_2 EFs were calculated for each SO_2 emission factor interval of Fig. 5. A linear trend was observed between the average particle and SO_2 EFs (Fig. 10). Coloured polygons represent results reported in literature, while the green circle marks the average as obtained with filter sampling. The slope of the linear regression, which is fitted to the EF results of the present study (black dots) may be interpreted as the EF of sulphate particles, while the intercept corresponds to the EF of other particle types (e.g. soot, organic, ash) at zero sulphur content.

However, it has been found that also the emission of organic particulate matter increases by higher rates of fuel sulphur content (Lack et al., 2009, 2011). This means that the slope of the regression line can be considered as the upper limit of sulphate particles, whose real EF can be lower depending on the ratio of organic particles.

It has to be noted that these sulphate and non-sulphuric particle EFs are averages over the measured fleet at given conditions. Sulphate and soot EFs depend on the combustion conditions, after treatment, engine load (Petzold et al., 2008, 2010), etc.; thus EFs for a particular ship can vary significantly. However, these EFs as average values can help to estimate the global particle emission of marine transportation.

It can be seen that Chen et al. (2005) and Sinha et al. (2003) published higher EF values from the vessel of *Royal Sphere* than that predicted from the regression line, while the other data of Sinha from the vessel of *MSC Giovanna* fits well to the

AMTD
5, 8925–8967, 2012

regression line. Higher EFs can be explained by different engine conditions and by differences in the characteristics of the measurement devices. For example, Sinha used a TSI 3025A CPC with a diameter range of 3–3000 nm, while the range of our TSI 3007 CPC was 10–1000 nm.

It is to be noted that some authors, like Hobbs et al. (2000), Petzold et al. (2008) and Murphy et al. (2009), observed lower particle EFs. This may also be due to different engine conditions or related to the measurement techniques. Murphy et al. (2009) reported that their CPCs, which had the same diameter range as ours, were saturated in the centre of the plume. This gives a possible explanation for the lower EF values reported by them.

The slope of the linear regression curve is 10^{15} particles per gram SO_2. Assuming that all of the fuel sulphur content is emitted as SO_2, this slope is equivalent to 2×10^{18} particles per 1 kg sulphur burnt, or $(s/100 \times \mathrm{kg\,fuel})^{-1}$, where s is the fuel sulphur content in percent. The intercept is $\sim 5 \times 10^{15}\,(\mathrm{kg\,fuel})^{-1}$, which may be used as an estimate of particle emissions at zero fuel sulphur content.

In order to assess the water-soluble ionic and elemental EF of ships, the aerosol samples were chemically analysed. Due to the difficulties of aerosol sampling (short time of plume passages), only two plume-background sample pairs were taken during the campaign. Since the amount of the aerosol collected during a single ship passage was very low, particles emitted by successive ships were accumulated on the same filter. The plumes of 51 and 75 ships were collected on the filters. The average CO_2 plume concentrations of the same ships were calculated, and subsequently, average ionic and metal EFs were derived.

Table 1 summarises the water-soluble ionic and metallic composition of the average plumes, calculated as a difference between the plume and the background concentrations.

The two filters show similar nitrate and sulphate EF. Comparing K^+, Ca^{2+}, V and Ni EFs with the fuel composition delivered by the chief engineer of Stena Line (Table 2), we find that they are at the same order of magnitude. Concerning Na, EF values were

AMTD
5, 8925–8967, 2012

20–50 times higher compared to the concentration in the fuel sample. This indicates the presence of an additional source apart from the fuel.

In Table 3 the sulphate EFs are compared to literature values. SO_2 and particle number (condensation nuclei or CN) EFs are also included. Particulate sulphur was compared to the total sulphur content of the fuel (forth column). From the SO_4^{2-} and CN EFs the mass median diameter (MMD) of sulphate particles was calculated by assuming spherical shaped particles with a density of 1.84 g cm^{-3}.

It can be concluded that we measured lower SO_4^{2-} EFs compared with the literature values, due to a lower sulphur content of the fuel used in SECA. Particulate sulphur to total fuel sulphur ratios are in the 4.26–5.56 % interval, except those from Moldanova et al. (2009), who reported a lower SO_4^{2-} EF. They performed the measurement in a cooled dilution system, in which sulphate may be lost through condensation (hence, the low EF).

The significant presence of sulphate aerosol in the fresh plume indicates fast oxidation of SO_2 to SO_3 that is promoted by high combustion temperature, as well as by oxidative catalyst systems.

The observed linear relationship between the fuel sulphur content and SO_4^{2-} EF is presented in Fig. 11. In addition to the three literature values for the high sulphur content domain (Agrawal, 2008; Petzold, 2008; Murphy, 2009), we present two values from the low sulphur content range. The points fit to a common regression line that describes the relationship between fuel sulphur content and SO_4^{2-} EF. As was discussed in the previous paragraph, Moldanova et al. might have lost a part of their sulphate, for that reason their value was ignored during the regression calculation.

The slope of the regression line indicates that 144 g SO_4^{2-} is produced for each kg sulphur that is burnt with the fuel. Lack et al. (2009) studied the relationship between fuel sulphur content and SO_4^{2-} EF on a statistically significant fleet. They obtained 140 g SO_4^{2-} per kg sulphur, which is in an excellent agreement with this value.

Combined with the number of particles produced from burning 1 kg sulphur with the fuel (2.0×10^{18}, i.e. the slope of Fig. 10) the average mass of particles could

AMTD
5, 8925–8967, 2012

be calculated. When assuming spherical particles of sulphuric acid with a density of 1.84 g cm^{-3}, the average mass could be converted to a MMD of 41.8 nm. This value is close to the MMD value that was directly calculated from the SO_4^{2-} and CN EFs for Sample B and Petzold's test rig data (Table 3), but only the half of the MMD that were calculated from Murphy's data. This indicates that this author might have underestimated the particle EF, as was previously assumed while discussing the results in Fig. 10.

At the same time, it has to be noted that we might overestimate the sulphate particle number from Fig. 10, which may refer to both sulphate and organic particles (see the discussion above of Fig. 10). It means that the ~ 42 nm can be seen as a lower limit for the diameter of sulphate particles.

3.3 NO_x emission factor

While the SO_2 and sulphate EFs depend on the fuel sulphur content, the NO_x EF mainly depends on the burning conditions of the engine and (slightly) on the fuel composition because heavy fuel oil contains some nitrogen-containing compounds (Nagai and Kawakami, 1989) that contribute to the NO_x emission.

The average NO_x EF was found to be 53.7 g (kg fuel)$^{-1}$ (NO_2 equivalent). Its distribution among the measured ships is shown in Fig. 12. The distribution is monomodal, Gaussian, with a maximum at 60 g (kg fuel)$^{-1}$. The majority of ships (more than 50 %) have a NO_x emission factor between 40–70 g (kg fuel)$^{-1}$.

This result is in accordance with NO_x emission factor calculations for different vessel types by the EDGARv4.2 based on the EMEP/EEA 2009 (CORINAIR) recommendations. The calculations yield an average NO_x emission factor of about 52 g (kg fuel)$^{-1}$.

The recent study of Williams et al. (2009) on a statistically significant fleet provides higher NO_x EF values. They measured at ~ 87 g (kg fuel)$^{-1}$ average EF for bulk carriers, while our value is ~ 43 g (kg fuel)$^{-1}$. Similarly, they measured significantly higher EF for tankers at ~ 79 g (kg fuel)$^{-1}$ versus our ~ 52 g (kg fuel)$^{-1}$. For container carriers,

AMTD
5, 8925–8967, 2012

passenger ships and tugs they measured at ~ 60 g (kg fuel)$^{-1}$, which is comparable to our 51 g (kg fuel)$^{-1}$.

The average NO_x EF was calculated and plotted in Fig. 13 against the crankshaft rpm (using the same bins as used before in Fig. 7). SDs per bins are also displayed. Ships for two strokes and four strokes engines are separated, because of the differences in the combustion conditions of the two types of engines. Since Tier I NO_x emission regulation has come into force in 2000, NO_x EFs are plotted separately for ships which are built (YoB) before and after 2000. No statistically significant differences could be observed between ships with a two strokes engine built before or after 2000. Therefore, the EFs for these ships were plotted together.

As for ships with four strokes engines, the NO_x EF for ships built before 2000 are higher than those which were built after 2000. The difference is especially significant within the low crankshaft rpm range (500–700 rpm).

A clearly decreasing trend in the NO_x EF could be observed with increasing crankshaft rpm. This is due to the fact that combustion takes more time in low speed engines than in faster engines, so a larger portion of nitrogen from air can be oxidised.

The molar NO_2-to-NO_x emission ratio, calculated from the mixing ratios of the two components in the plume (%, n/N), is presented in Fig. 14. As can be seen, nitrogen oxides are mostly emitted as NO, the ratio of NO_2 emission is less than 25 % at the majority of the ships.

As Fig. 15 demonstrates, the NO_2-to-NO_x emission ratio does not depend on the ambient ozone concentration that indicates that the oxidation of NO to NO_2 in the fresh plume was probably of little importance. In the figure, diurnal averages NO_2-to-NO_x ratios were calculated and plotted for the plume and ambience separately. Diurnal averages of ozone concentrations are plotted as well. The hourly average concentrations of ambient atmospheric trace gases were provided by the air quality monitoring station operated by the local authority (DCMR Environmental Protection Agency, Rijnmond, Port of Rotterdam) in the 20 m vicinity of the sampling location at Hoek van

AMTD
5, 8925–8967, 2012

Holland. Using the hourly averages, diurnal averages were created considering the periods where plume measurements were taken (between 08:00 and 20:00 LT).

It can be seen that the ambient NO_2-to-NO_x ratio correlates with the ozone concentration, while the plume ratio oscillates between 15 and 40 % independently of the ozone concentration. This indicates that the more oxidative atmosphere results in a higher NO_2 ambient ratio at larger scales, while it does not significantly affect the composition of the fresh plume.

4 Summary and conclusions

A ship emission survey on a statistically relevant fleet has been reported. The plumes of the passing ships were measured at the entrance of the port of Rotterdam (Hoek van Holland). The concerned components were SO_2, NO, NO_2 and particulate matter. The CO_2 concentrations in the plumes were measured in order to normalize the emission factors for fuel consumption.

4.1 Gaseous emission factors

Distributions of SO_2, NO_x and particulate matter EFs were calculated according to ship duty type, main engine power and crankshaft rotational speed. Inland vessels, port service boats, and sea duty ships form a discrete SO_2 EF group. No significant differences were found between SO_2 EFs of two stroke and four stroke engines. A clearly increasing trend was found for SO_2 EF with the engine power of the ships, possibly due to a decreased relative contribution of auxiliary engine emissions on high powered ships.

The average NO_x EF was found to be $\sim 54\,\mathrm{g\,(kg\,fuel)^{-1}}$ which is in agreement with the EDGARv4.2 database. The NO_x EF decreases with an increasing crankshaft rotational speed, which might be explained by the shorter residence time of a given air

AMTD
5, 8925–8967, 2012

volume in the combustion space. Significantly lower NO_x EFs were found for ships built after 2000, fulfilling Tier I regulation of MARPOL.

It was found that nitrogen oxides were emitted mainly as NO, while the NO_2 emission was around 20 % of the NO_x emission. This ratio did not depend on the ambient ozone concentration, while ambient NO_2-to-NO_x emission ratio correlated with ozone concentration. This indicates that the ozone driven NO-NO_2 conversion requires more time before it significantly influences the composition of the fresh plume.

4.2 Emission factors for particles and sulphate

A linear relationship was found between the SO_2 EF (or fuel S content) and the particle number EF. The slope of the regression line shows that on average about 2×10^{18} particles are formed with 1 kg sulphur burnt, while the intercept indicates that about 5×10^{15} non-sulphuric particles (soot, ash, etc.) are emitted with 1 kg fuel burnt at zero sulphur content.

The filter sulphate measurements represented ships which are powered by fuel with a low sulphur content (less than 1 %), while other authors reported results for high sulphur contents (2–3 % fuel S). However, both were found to be proportional with the corresponding fuel sulphur ratio. The proportionality factor was found to be 144 g sulphate per 1 kg sulphur burnt with the fuel. This means that ~ 4.8 % of the total sulphur content emitted in particle form (i.e. sulphate), or transformed to particulate form immediately after emission from the stack.

The mass median diameter of sulphate particles was estimated from the particle number and sulphate EFs as ~ 42 nm.

4.3 Outlook

The global average of fuel sulphur content composed by SECA and non-SECA zones was 2.2 % for the year 2000 according to Eyring et al. (2010). This value will decrease in the future according the sulphur content regulations in SECA and non-SECA.

AMTD
5, 8925–8967, 2012

Assuming that the traffic distribution between the zones will not change, the average sulphur content will follow the trend plotted in Fig. 1 (black line). Applying global fuel consumption data for the year 2001 according to Eyring et al. (2005) the annual SO_2 emission of marine traffic can be calculated. This value can be transformed to annual SO_4^{2-} emission using the slope of Fig. 11. The obtained 792 Gg/y agrees with Eyring's 785 Gg/y value (Eyring et al., 2005). In contrary Lack et al. (2009) estimated a significant lower value at 412 Gg/y.

The predicted variation of the SO_4^{2-} annual emission over the coming years is presented in Fig. 1. We emphasise that in addition to the direct emission SO_4^{2-} an important contribution to sulphate aerosols in the marine troposphere comes from the oxidation of SO_2 emitted by ships.

It can be also concluded that the remote (e.g. from the shore) analysis of plume composition could be an efficient tool in hands of authorities to check the sulphur limit compliance of the ships.

Acknowledgements. The authors would like to acknowledge the collaboration with Stena Line and in particular the support from the chief engineer Dick Van Der Ent. The Dutch agency DCMR are thanked for providing ozone concentration data from the station. Finally we thank The European Commission, DG Environment, for financing the project "Remote surveillance of ship emissions of sulphur dioxide" which provided the framework for the present study. SDG.

References

Agrawal, H., Malloy, Q. G. J., Welch, W. A., Miller, J. W., and Cocker, D. R.: In-use gaseous and particulate matter emissions from a modern ocean going container vessel, Atmos. Environ., 42, 5504–5510, 2008.

Berg, N., Mellqvist, J., Jalkanen, J.-P., and Balzani, J.: Ship emissions of SO_2 and NO_2: DOAS measurements from airborne platforms, Atmos. Meas. Tech., 5, 1085–1098, doi:10.5194/amt-5-1085-2012, 2012.

AMTD
5, 8925–8967, 2012

Chen, G., Huey, L. G., Trainer, M., Nicks, D., Corbett, J., Ryerson, T., Parrish, D., Neumann, J. A., Nowak, J., Tanner, D., Holloway, J., Brock, C., Crawford, J., Olson, J. R., Sullivan, A., Weber, R., Schauffler, S., Donnelly, S., Atlas, E., Roberts, J., Flocke, F., Hubler, G., and Fehsenfeld, F.: An investigation of the chemistry of ship emission during ITCT 2002, J. Geophys. Res., 110, D10S90, doi:10.1029/2004JD005236, 2005.

Cofala, J., Amann, M., Heyes, C., Klimont, Z., Posch, M., Schopp, W., Tarasson, L., Jonson, J., Whall, C., and Stavrakaki, A.: Final Report: Analysis of Policy Measures to Reduce Ship Emissions in the Context of the Revision of the National Emissions Ceilings Directive, March 2007, International Institute for Applied Systems Analysis, Laxenburg, Austria, p. 74, 2007.

Cohen, A. J., Anderson, H. R., Ostro, B., Pandey, K. D., Krzyzanowski, M., Kunzli, N., Gutschmidt, K., Pope, A., Romieu, I., Samet, J. M., and Smith, K.: The global burden of disease due to outdoor air pollution, J. Toxicol. Environ. Heal. A, 68, 1301–1307, 2005.

Cooper, D. A.: HCB, PCB, PCDD and PCDF emissions from ships, Atmos. Environ., 39, 4901–4912, 2005.

Corbett, J. J., Winebrake, J. J., Green, E. H., Kasibhatla, P., Eyring, V., and Lauer, A.: Mortality from ship emissions: a global assessment, Environ. Sci. Technol., 41, 8512–8518, 2007.

Dalsøren, S. B., Eide, M. S., Endresen, Ø., Mjelde, A., Gravir, G., and Isaksen, I. S. A.: Update on emissions and environmental impacts from the international fleet of ships: the contribution from major ship types and ports, Atmos. Chem. Phys., 9, 2171–2194, doi:10.5194/acp-9-2171-2009, 2009.

Duyzer, J., Hollander, K., Verhagen, H., Weststrate, H., Hensen, A., Kraai, A., and Koos, G.: Assessment of emissions of PM and NO_x of sea going vessels by field measurements, TNO report no. 2006-A-R0341/B, 2006.

Endersen, Ø., Sorgard, E., Behrens, H. L., Brett, P. O., and Isaksen, I. S. A.: A historical reconstruction of ships' fuel consumption and emissions, J. Geophys. Res., 112, D12301, doi:10.1029/2006JD007630, 2007.

European Commission, Joint Research Centre, Netherlands Environmental Assessment Agency: Emission Database for Global Atmospheric Research (EDGAR), release version 4.2, available at: http://edgar.jrc.ec.europa.eu (last access: December 2012), 2011.

Eyring, V., Kohler, H. W., van Aardenne, J., and Lauer, A.: Emissions from international shipping: 1. The last 50 years, J. Geophys. Res., 110, D17305, doi:10.1029/2004JD005619, 2005.

AMTD
5, 8925–8967, 2012

Eyring, V., Isaksen, I. S. A., Berntsen, T., Collins, W. J., Corbett, J. J., Endresen, Ø., Grainger, R. G., Moldanova, J., Schlager, H., and Stevenson, D. S.: Transport Impacts on Atmosphere and Climate: Shipping, Atmos. Environ., 44, 4735–4771, 2010.

Hobbs, P. V., Garrett, T. J., Ferek, R. J., Strader, S. R., Hegg, D. A., Frick, G. M., Hoppel, W. A., Gasparovic, R. F., Russell, L. M., Johnson, D. W., O'Dowd, C., Durkee, P. A., Nielsen, K. E., and Innis, G.: Emissions from ships with respect to their effects on clouds, J. Atmos. Sci., 57, 2570–2590, 2000.

IPCC: Climate change 2007: impacts, adaptation and vulnerability. Contribution of Working Group II to the Fourth Assessment Report of the Intergovernmental Panel on Climate Change, edited by: Parry, M. L., Canziani, O. F., Palutikof, J. P., van der Linden, P. J., and Hanson, C. E., Cambridge University Press, Cambridge, UK, p. 976, 2007.

Lack, D. A., Corbett, J. J., Onasch, T., Lerner, B., Massoli, P., Quinn, P. K., Bates, T. S., Covert, D. S., Coffman, D., Sierau, B., Herndon, S., Allan, J., Baynard, T., Lovejoy, E., Ravishankara, A. R. and Williams, E.: Particulate emissions from commercial shipping: Chemical, physical, and optical properties, J. Geophys. Res., 114, D00F04, doi:10.1029/2008JD011300, 2009.

Lack, D. A., Cappa, C. D., Langridge, J., Bahreini, R., Buffaloe, G., Brock, C., Cerully, K., Coffman, D., Hayden, K., Holloway, J., Lerner, B., Massoli, P., Li, S. M., McLaren, R., Middlebrook, A. M., Moore, R., Nenes, A., Nuaaman, I., Onasch, T. B., Peischl, J., Perring, A., Quinn, P. K., Ryerson, T., Schwartz, J. P., Spackman, R., Wofsy, S. C., Worsnop, D., Xiang, B., and Williams, E.: Impact of Fuel Quality Regulation and Speed Reductions on Shipping Emissions: Implications for Climate and Air Quality, Environ. Sci. Technol., 45, 9052–9060, doi:10.1021/es2013424, 2011.

Mellqvist, J. and Berg, N.: Identification of Gross Polluting Ships, Final report to Vinnova: RG Report (Göteborg) No. 4, ISSN 1653 333X, Chalmers University of Technology, 2010.

Mellqvist, J. and Berg, N.: Airborne surveillance of sulphur and NO_x in ships as a tool to enforce IMO legislation, Atmos. Meas. Tech. Discuss., in preparation, 2012.

Mellqvist, J., Berg, N., and Ohlsson, D.: Remote surveillance of the sulfur content and NO_x emissions of ships, Second international conference on Harbours, Air Quality and Climate Change (HAQCC) 2008, Rotterdam, 2008.

Moldanova, J., Fridell, E., Popovicheva, O., Demirdjian, B., Tishkova, V., Faccinetto, A., and Focsa, C.: Characterisation of particulate matter and gaseous emissions from a large ship diesel engine, Atmos. Environ., 43, 2632–2641, 2009.

AMTD
5, 8925–8967, 2012

Murphy, S. M., Agrawal, H., Sorooshian, A., Padro, L. T., Gates, H., Hersey, S., Welch, W. A., Jung, H., Miller, J. W., Cocker, D. R., Nenes, A., Jonsson, H. H., Flagan, R. C., and Seinfeld, J. H.: Comprehensive simultaneous shipboard and airborne characterisation of exhaust from a modern container ship at sea, Environ. Sci. Technol., 43, 4626–4640, 2009.

Nagai, T. and Kawakami, M.: Reduction of NO_x Emission in Medium-speed Diesel Engines, Society of Automotive Engineers, 1989.

Petzold, A., Hasselbach, J., Lauer, P., Baumann, R., Franke, K., Gurk, C., Schlager, H., and Weingartner, E.: Experimental studies on particle emissions from cruising ship, their characteristic properties, transformation and atmospheric lifetime in the marine boundary layer, Atmos. Chem. Phys., 8, 2387–2403, doi:10.5194/acp-8-2387-2008, 2008.

Petzold, A., Weingartner, E., Hasselbach, J., Lauer, A., Kurok, C., and Fleischer, F.: Physical Properties, Chemical Composition, and Cloud Forming Potential of Particulate Emissions from a Marine Diesel Engine at Various Load Conditions, Environ. Sci. Technol., 44, 3800–3805, 2010.

Segers, A. and Duyzer, J. H.: Ratio of SO_2/CO_2 from ships emission, TNO internal report, 2007.

Sinha, P., Hobbs, P. V., Yokelson, R. J., Christian, T. J., Kirckstetter, T. W., and Bruintjes, R.: Emissions of trace gases and particles from two ships in the southern Atlantic Ocean, Atmos. Environ., 37, 2139–2148, 2003.

Whall, C., Stavrakaki, A., Ritchie, A., Green, C., Shialis, T., Minchin, W., Cohen, A., and Stokes, R.: Ship emissions inventory – Mediterranean Sea, CONCAWE Final Report, Entec UK Limited, London, England, 2007.

Williams, E. J., Lerner, B. M., Murphy, P. C., Herndon, S. C., and Zahniser, M. S.: Emissions of NO_x, SO_2, CO and HCHO from commercial marine shipping during Texas Air Quality Study (TexAQS) 2006, J. Geophys. Res., 114, D21306, doi:10.1029/2009JD012094, 2009.

AMTD
5, 8925–8967, 2012

Table 1. Average EF of metal and water-soluble ionic components of aerosols observed in ship plumes. The unit is mg (kg fuel)$^{-1}$.

	NO_3^-	SO_4^{2-}	Cl^-	Na^+	NH_4^+	K^+	Mg^{2+}	Ca^{2+}	V^*	Ni^*
Sample A	150 ±10	570 ±30	180 ±10	180 ±10	170 ±10	10 ±1	20 ±2	70 ±7	35 ±7	22 ±4
Sample B	190 ±10	390 ±20	380 ±10	490 ±20	60 ±10	10 ±1	40 ±4	50 ±5	16 ±3	11 ±2

* Determined by XRF analysis.

AMTD
5, 8925–8967, 2012

Table 2. Elemental composition of a fuel sample delivered by the chief engineer of Stena Line.

	concentration mg (kg fuel)$^{-1}$
Vanadium (V)	34 ± 2
Nickel (Ni)	20 ± 1
Calcium (Ca)	16 ± 0.8
Potassium (K)	1 ± 0.05
Sodium (Na)	10 ± 0.5

AMTD
5, 8925–8967, 2012

Table 3. Emission factors (EF) for SO_2, SO_4^{2-}, and particulate matter (CN). Particulate sulphur ratios to the total fuel sulphur content were calculated from the SO_4^{2-} to SO_2 EF ratios. Mass median diameters (MMD) were calculated from the SO_4^{2-} and CN EFs ratio assuming spherical particle shape and 1.84 g cm^{-3} density.

	Fuel S, %	SO_2 EF, g (kg fuel)$^{-1}$	SO_4^{2-} EF, g (kg fuel)$^{-1}$	Particle S /Fuel S, %	CN EF 10^{16}, (kg fuel)$^{-1}$	MMD, nm
Sample A	0.32 ± 0.07	6.5 ± 1.5	0.57 ± 0.03	5.56	n.a.	n.a.
Sample B	0.29 ± 0.07	5.9 ± 1.4	0.39 ± 0.02	4.26	1.05 ± 0.1	42.2[e]
Petzold (test rig)	2.21[a]	44.2	2.89[d]	4.27	2.17[a,b]	52.1
Murphy (in stack)	2.98	59.7[a]	4.30[a]	4.58	1.3[a]	80.9
Agrawal (2008)	2.05[a]	41.0	3.24[c]	5.16	n.a.	n.a.
Moldanova	1.95[a]	39.0	0.76[a]	1.28	n.a.	n.a.

Note: n.a.– not available,
[a] – original data taken from reference,
[b] – difference of numbers of total particles and non-volatile particles,
[c] – converted from g kW^{-1} h^{-1} data using CO_2 EF,
[d] – converted from mg sm^{-3} data using CO_2 mixing ratio,
[e] – sulphate particle concentration was considered as the difference of CN and the interception of Fig. 10.

AMTD
5, 8925–8967, 2012

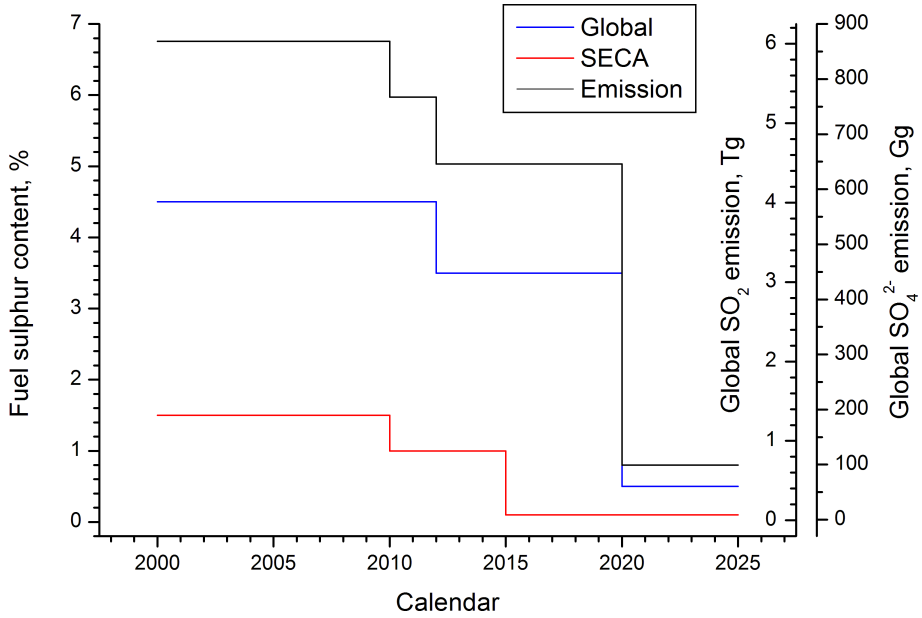

Fig. 1. Timeline for the reduction of sulphur content in fuels, globally and in SECAs. Calculated and predicted global SO_2 and SO_4^{2-} emission are also plotted in accordance with the change of the estimated global average of fuel sulphur content.

AMTD
5, 8925–8967, 2012

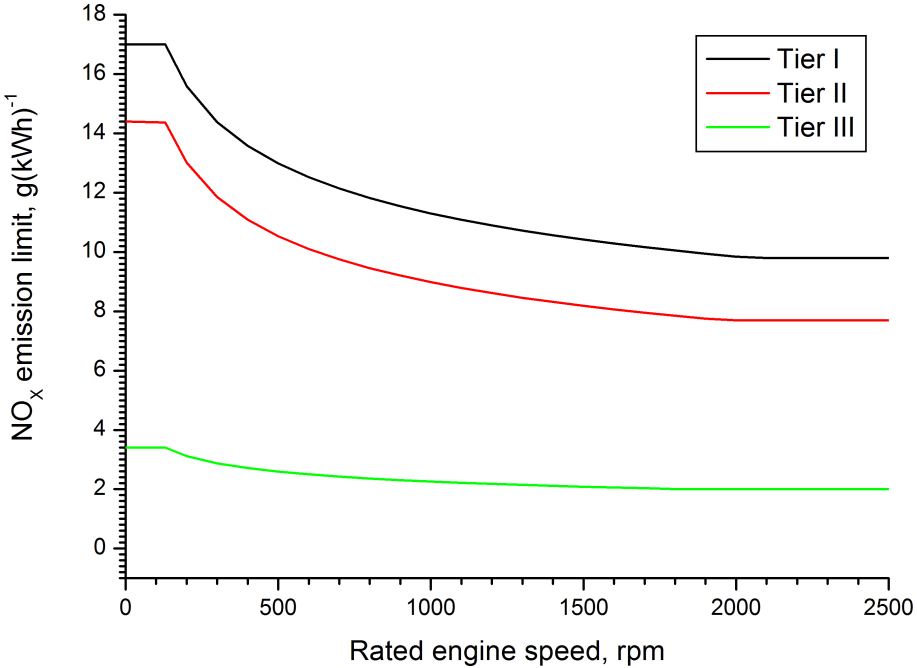

Fig. 2. NO_x emission limits, at different rated engine speeds, for ships built after 2000 (Tier I), after 2011 (Tier II), and after 2016 in emissions control areas (Tier III).

AMTD
5, 8925–8967, 2012

Fig. 3. Map of the measurement area, with marks at the 3 measurement sites. HvH – Hoek van Holland, LG – Landtong, ME – Maasvlakte.

AMTD
5, 8925–8967, 2012

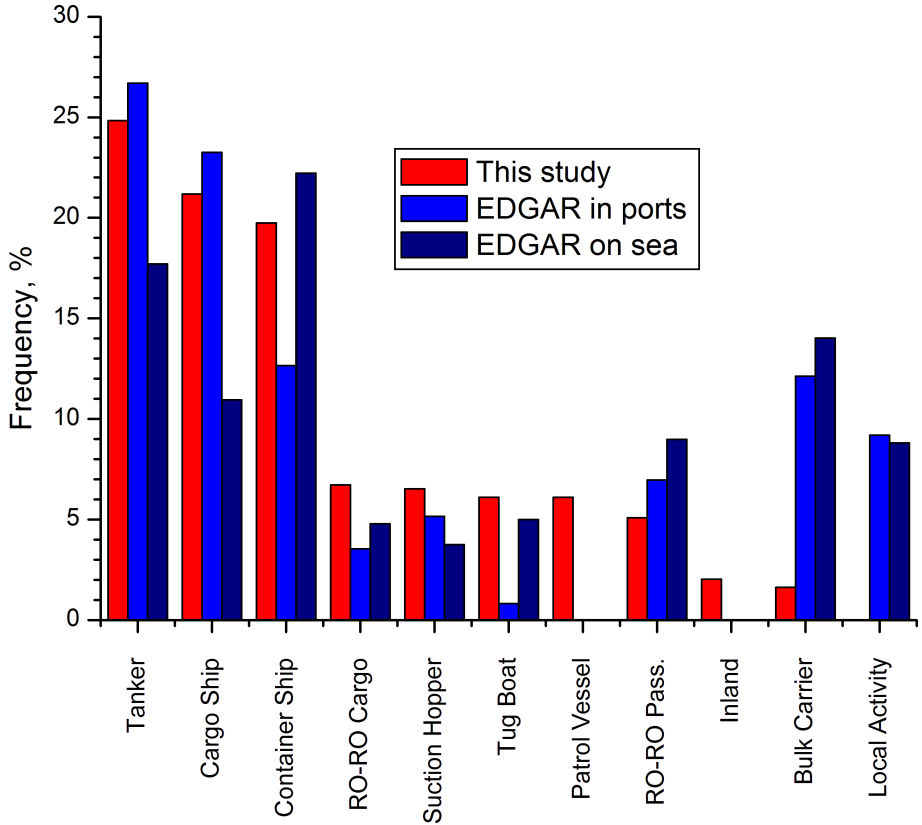

Fig. 4. Distribution of the studied ships according to duty, compared with EDGARv4.2 database.

AMTD
5, 8925–8967, 2012

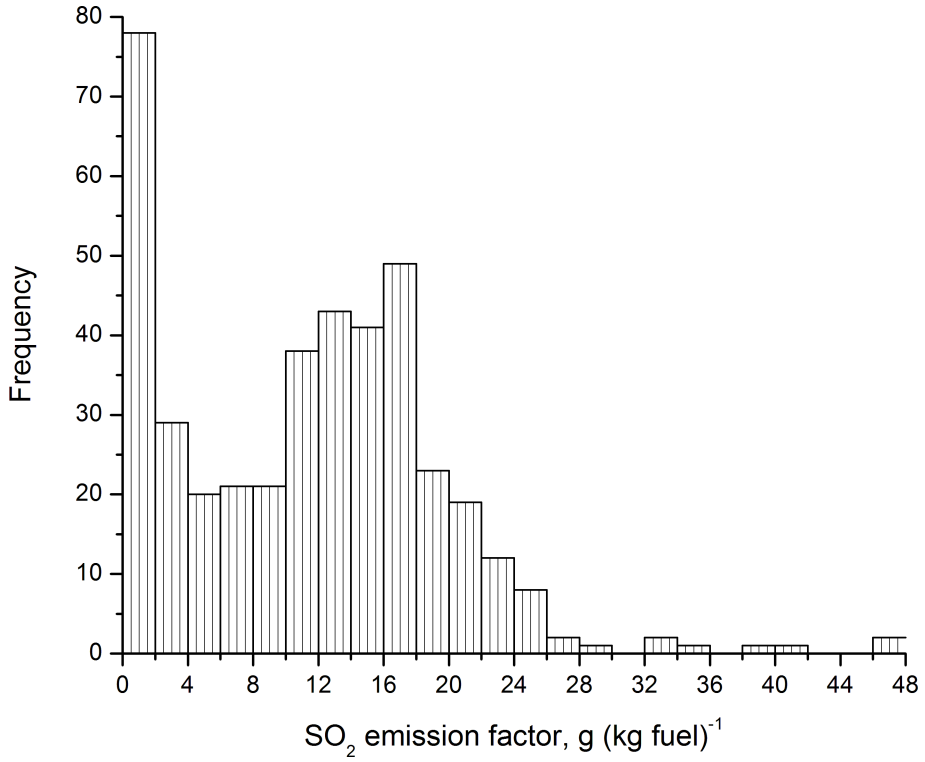

Fig. 5. Distribution of the SO_2 emission factors of the ships under study. The total SO_2 EF range was divided into 24 EF bins. Frequencies of the EF bins are plotted along the y-axes.

.

AMTD
5, 8925–8967, 2012

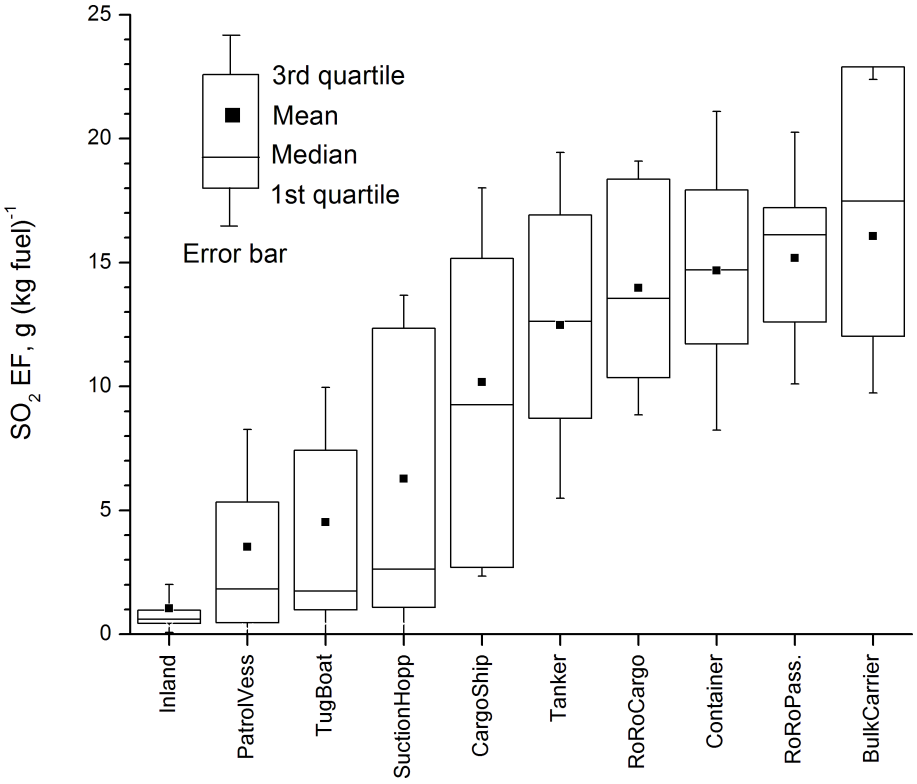

Fig. 6. SO_2 EF distribution among duty type of the ships.

AMTD
5, 8925–8967, 2012

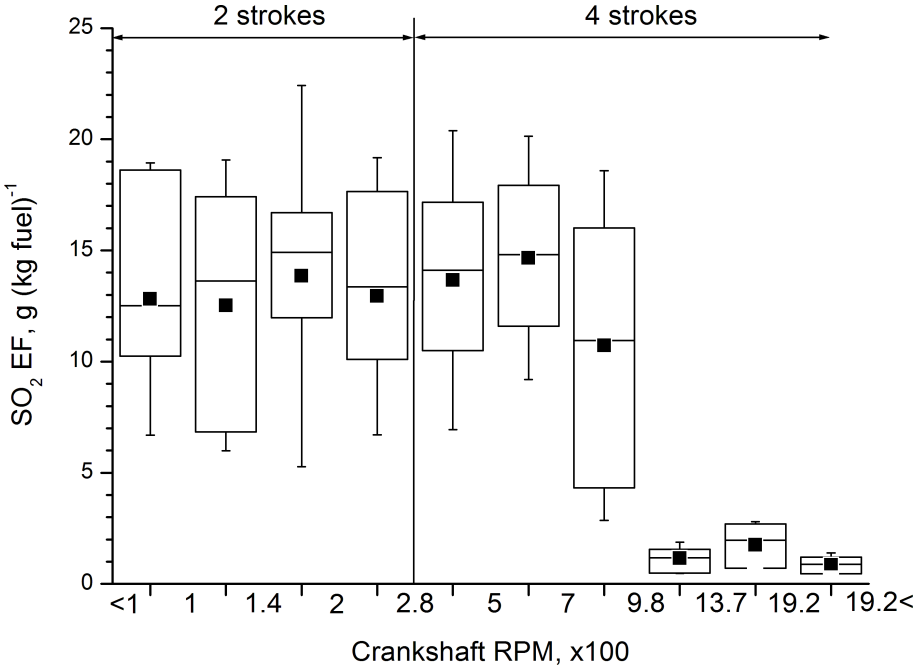

Fig. 7. SO_2 EF distribution among crankshaft rpm of the engine. The crankshaft range was divided into 11 bins based on logarithmic scale. Average SO_2 EFs of the bins are plotted along the y-axes, while sticks on the x-axes refer the borders of the bins.

AMTD
5, 8925–8967, 2012

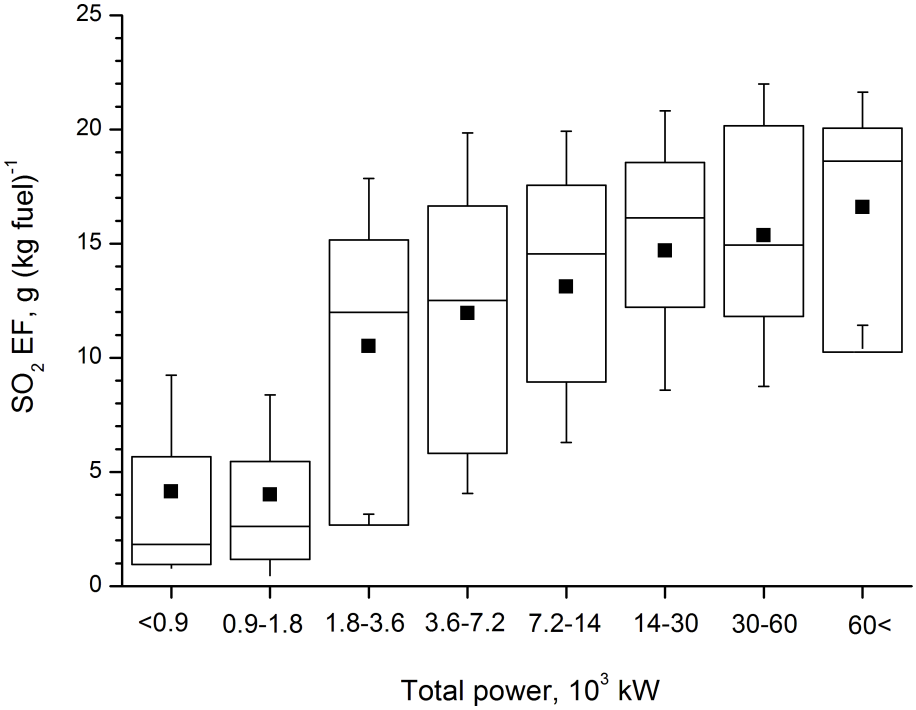

Fig. 8. The SO_2 EF distribution with the engine power of the ships. The power range of the ships was divided into 8 intervals based on logarithmic scale. Average SO_2 EFs of the bins are plotted along the y-axes, while power bins are marked on the x-axes.

AMTD
5, 8925–8967, 2012

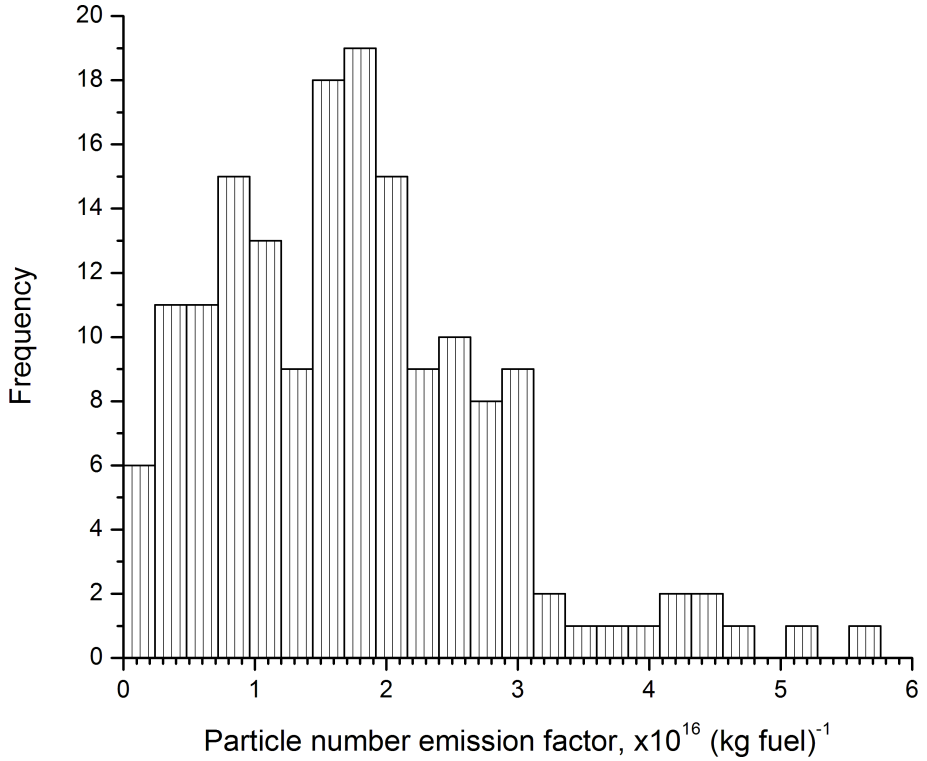

Fig. 9. Distribution of particle emission factors of the studied ships. The total particle EF range was divided into 24 EF bins. Frequencies of the EF bins are plotted along the y-axes.

AMTD
5, 8925–8967, 2012

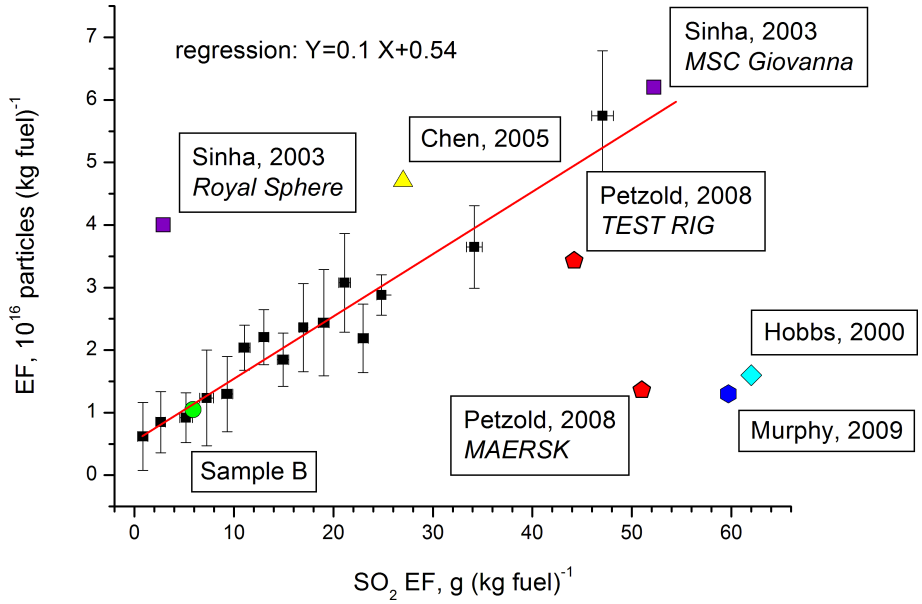

Fig. 10. Particle emission factor as a function of SO_2 EF (black dots). Literature data are represented by coloured polygons. Error bars represent standard deviations. Slope of the regression line: 0.1 ± 0.014, intercept: 5.4 ± 2.0, R^2 : 0.95.

AMTD
5, 8925–8967, 2012

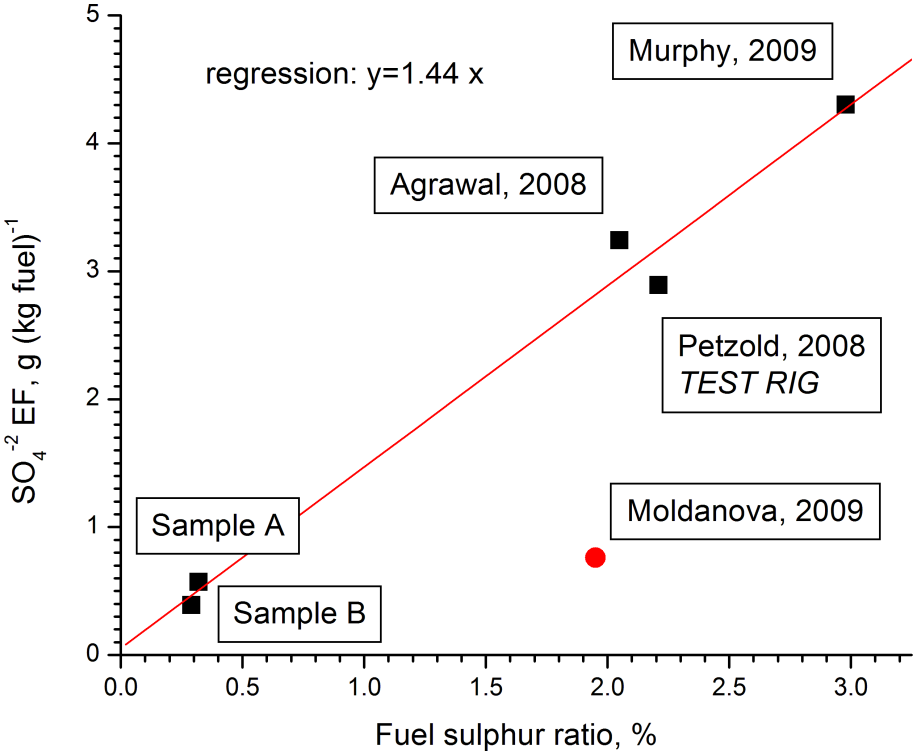

Fig. 11. The SO_4^{2-} EF as a function of fuel sulphur ratio. Red dot marks an outlier that was ignored during the regression calculation. Slope of the regression line: 1.44 ± 0.1, intercept forced to be zero, R^2 : 0.98.

AMTD
5, 8925–8967, 2012

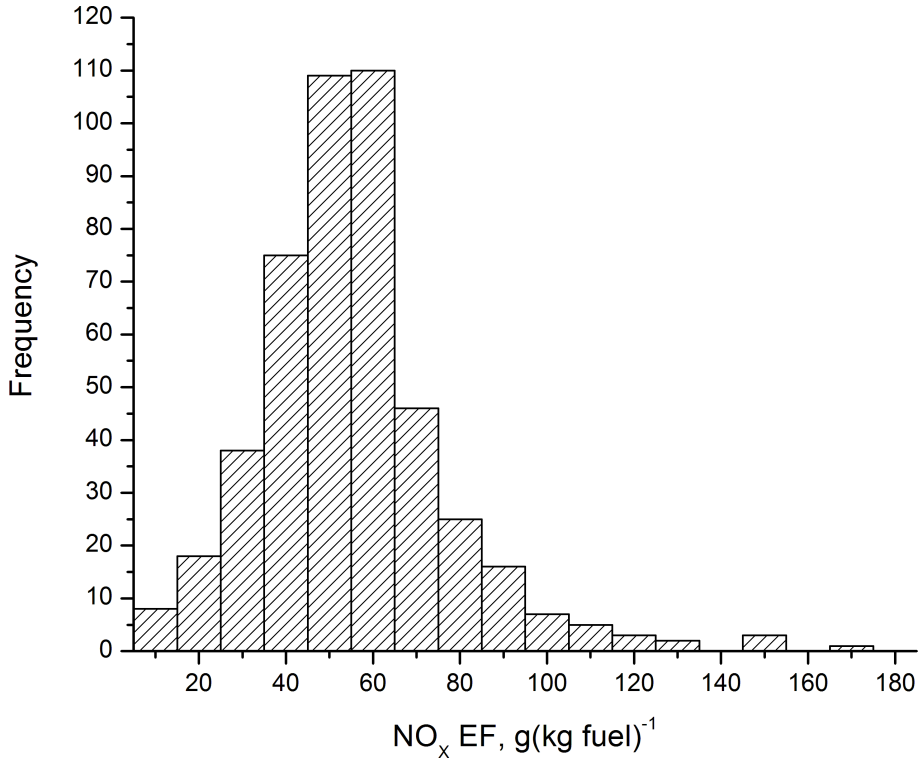

Fig. 12. Distribution of the NO_x emission factor among the measured ships. The total NO_x EF range was divided into 18 EF bins. Frequencies of the EF bins are plotted along the y-axes. NO_x EF values are represented as NO_2 equivalent.

AMTD
5, 8925–8967, 2012

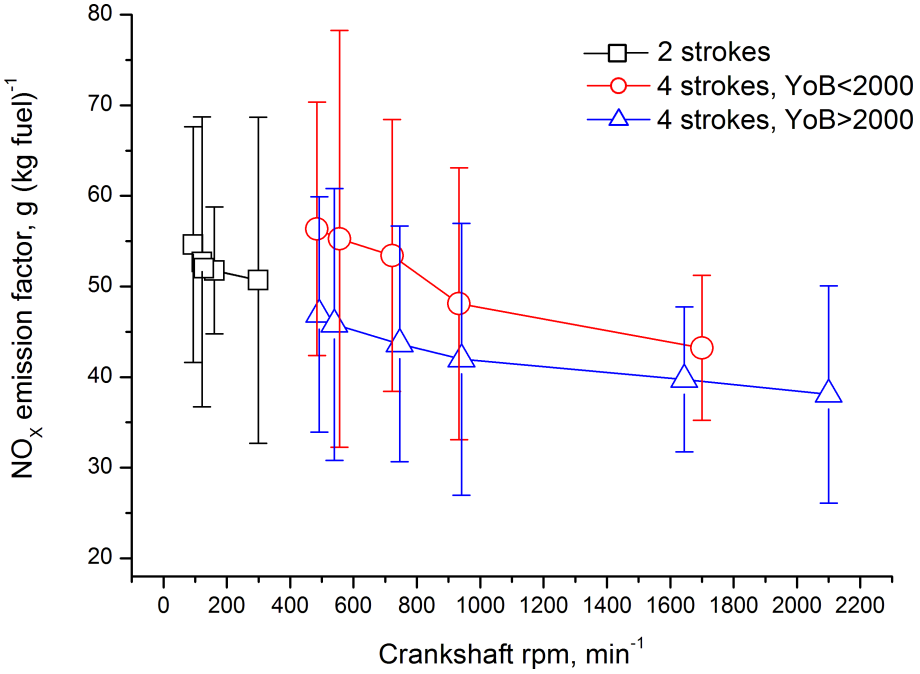

Fig. 13. The NO_x EF against crankshaft rpm. Values for two strokes engines and four strokes engines built before and after year 2000 were plotted in different colours. Error bars refer the standard deviations of NO_x EF in RPM bins. NO_x EF values are represented as NO_2 equivalent.

AMTD
5, 8925–8967, 2012

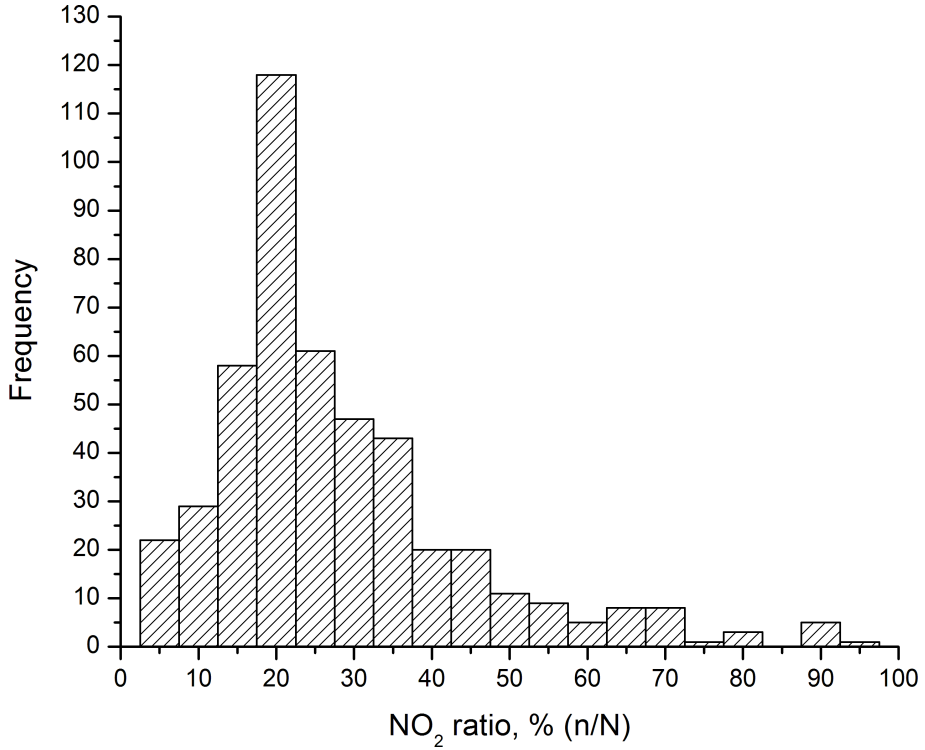

Fig. 14. Distribution of the NO_2/NO_x molar ratio among the studied ships. The total molar ratio range was divided into 19 bins. Frequencies of the bins are plotted along the y-axes.

AMTD
5, 8925–8967, 2012

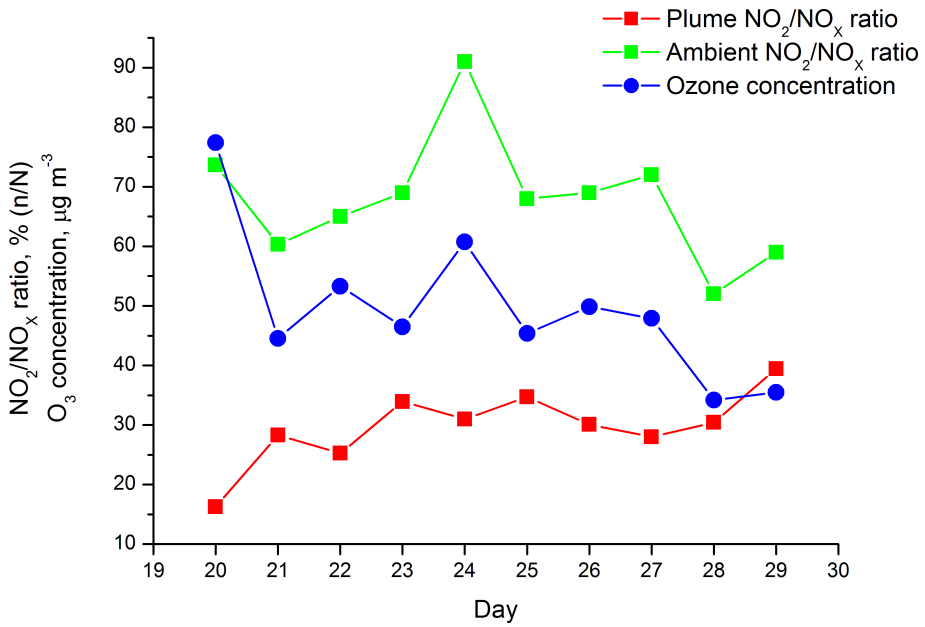

Fig. 15. Diurnal averages of ambient and plume NO_2/NO_x molar ratios and ozone concentrations during the measurement campaign. Concentration data between 08:00 and 20:00 were concerned for the averaging.

AMTD
5, 8925–8967, 2012